Mathematical Modeling, Experimental Validation and Observer Design for a Capacitively Actuated Microcantilever

Mariateresa Napoli[1] Bassam Bamieh[2] Kimberly Turner[3]

Department of Mechanical Engineering,
University of California,
Santa Barbara, CA 93106,
U.S.A.

Abstract

We present a mathematical model for the dynamics of an electrostatically actuated micro-cantilever. For the common case of cantilevers excited by a periodic voltage, we show that the underlying linearized dynamics are those of a periodic system described by a Mathieu equation. We present experimental results that confirm the validity of the model, and in particular, illustrate that parametric resonance phenomena occur in capacitively actuated microcantilevers. We propose a system where the current measured is used as the sensing signal of the cantilever state and position through a dynamical observer. By investigating how the best achievable performance of an optimal observer depends on the excitation frequency, we show that the best such frequency is not necessarily the resonant frequency of the cantilever.

1 Introduction

The recent advances in the field of miniaturization and microfabrication have paved the way for a new range of applications, bringing along the promise of unprecedented levels of performance, attainable at a limited cost, thanks to the use of batch processing techniques.

In particular, scanning probe devices have proven to be extremely versatile instruments, with applications that range from surface imaging at the atomic scale, to ultra high density data storage and retrieval, to biosensors, and to nanolithography.

However, in order to achieve the anticipated results in terms of performance, an increase in throughput is required. In this respect, much of the research effort has been focused on the design of integrated detection schemes, which offer moreover the advantage of compactness.

The most common solutions make use of the piezoresistive [5, 15], piezoelectric [6, 8, 10], thermal expansion [7] or capacitive effects [1, 3, 14]. The device that we propose is an electrostatically actuated microcantilever. More precisely, in our design the microcantilever constitutes the movable plate of a capacitor and its displacement is controlled by the voltage applied across the plates.

A major advantage of capacitive detection, is the fact that it offers both electrostatic actuation as well as integrated detection, without the need for an additional position sensing device. The common scheme used in capacitive detection is to apply a second AC voltage at a frequency much higher than the mechanical bandwidth of the cantilever. The current output at that frequency is then used to estimate the capacitance, and consequently the cantilever's position. This sensing scheme is the simplest position detection scheme available, however, it is widely believed to be less accurate than optical levers or piezoresistive sensing. We propose a novel scheme that avoids the use of a high frequency probing signal by the use of a dynamical state observer whose input is the current through the capacitive cantilever. For the purpose of implementation, this scheme offers significant advantages as it involves simpler circuitry. By using an optimal observer, or by tuning the observers gains, it is conceivable that a high fidelity position measurement can be obtain, thus improving resolution in atomic force microscopy applications.

In this paper, we present a model for this electrostatically actuated microcantilever. Using simple parallel plate theory and for the common case of sinusoidal excitation, it turns out that its dynamics are governed by a special second order linear periodic differential equation, called the Mathieu equation. We produce experimental evidence that validates the mathematical model, including a mapping of the first instability region of the Mathieu equation.

The optimal observer problem that was formulated also in [12] is solved here following a different and simpler approach. This optimal design is then used as an analysis tool to select the frequency of excitation that corresponds to the best achievable observer performance. In other words, the optimal observer design is used to actually design the system (rather than the observer), by selecting the excitation frequency that produces the least estimation error. Inter-

[1]e-mail: napoli@engineering.ucsb.edu
[2]e-mail: bamieh@engineering.ucsb.edu.
[3]e-mail: turner@engineering.ucsb.edu.

0-7803-7896-2/03/$17.00 ©2003 IEEE

Proceedings of the American Control Conference
Denver, Colorado June 4-6, 2003

estingly, it turns out that this frequency is not necessarily the resonant frequency of the cantilever, and it depends on the statistics of the measurement and process noise.

After the optimal excitation frequency is selected, we design a suboptimal reduced order observer, whose parameters are tuned to match the optimal performance index as close as possible. The extension of these results to the array configuration is the subject of our current research.

The paper is organized as follows: In Section 2 we develop the mathematical model of an electrostatically actuated cantilever. In Section 3 we present the experimental results that validate the model including, in particular, the mapping of the first instability region of the Mathieu equation. In Section 4 we pose the optimal observer problem for time varying systems and in Section 5 we design a suboptimal reduced order observer. Finally, we present our conclusions in Section 6.

2 Model Description For a Single Cantilever

The schematic of a single cantilever sensor is shown in Fig.1. It consists of two adjacent electrically conductive beams forming the two plates of a capacitor. One of the beams is rigid, while the other (hereafter referred to as the cantilever) is fairly soft and represents the movable part of the structure.

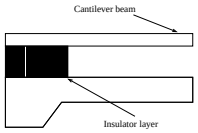

Figure 1: A schematic of an electrostatically driven cantilever.

If the length of the cantilever is much bigger than its distance from the bottom plate, the capacitance is given by

$$C(x) = \frac{\epsilon_o A}{d - z},$$

where $\epsilon_o = 8.85\ 10^{-12} As/Vm$ is the permittivity in vacuum, A is the area of the plates, d is the gap between them and z is the vertical displacement of the cantilever from its rest position.

The attractive force, F_a, between the capacitor plates generated by applying a voltage $V(t)$, can be easily found to be

$$F_a = \frac{1}{2}\frac{\epsilon_o A}{d^2}\frac{V^2(t)}{(1-\frac{z}{d})^2} \approx \frac{1}{2}\frac{\epsilon_o A}{d^2}(1+2\frac{z}{d})V^2(t),$$

where the approximation holds when $\frac{z}{d} << 1$.

Only few algebraic steps are sufficient to derive the equation of motion of the cantilever, which if $V(t) = V_o \cos\omega_o t$, is given by

$$z'' + cz' + (a - 2q\cos 2t)z = u_f(t), \qquad (1)$$

where the prime denotes the derivative with respect to the scaled time $\tau = \omega_o t$; c is a small damping coefficient, both from air friction and structural losses, $a = \frac{k}{m\omega_o^2} - \frac{1}{2}\frac{\epsilon_o A V_o^2}{md^3\omega_o^2}$, k is the spring constant of the cantilever, $q = \frac{\epsilon_o A V_o^2}{4md^3\omega_o^2}$, and $u_f(t) = q\,d\cos^2(t)$.

Equation (1) is an instance of the well-known Mathieu equation. Its properties are briefly discussed in the next section. Here we just point out that when $u_f(t) \equiv 0$, this equation has very peculiar stability properties, that have been extensively investigated. As a and q vary in $\mathbf{R}$, its stable solutions can be periodic, but they never decay to zero. In the case of our interest, where $u_f(t) \neq 0$ and periodic, we can prove that, for any pair of parameters a and q, the forced equation retains the same stability properties as the unforced one.

We consider the current generated as the output y of the system. Its first order approximation is given by

$$y = c_1(t)z + c_2(t)z' + v_f(t), \qquad (2)$$

where $c_1(t) = -\frac{\epsilon_o A V_o w_o}{d^2}\sin t$, $c_2(t) = \frac{\epsilon_o A V_o}{d^2}\cos t$, and $v_f(t) = \frac{\epsilon_o A V_o w_o}{d}\sin t$.

Introducing the vector $x = [z \quad \dot{z}]^T$, we can derive from (1) and (2) the state space representation of the cantilever model

$$\begin{array}{c} x' = A(t)x + B(t)u_f(t) \\ y = C(t)x + v_f(t), \end{array} \qquad (3)$$

where $A(t) = \begin{bmatrix} 0 & 1/w_o \\ -a + 2q\cos 2t & -c \end{bmatrix}$; $B = \begin{bmatrix} 0 \\ 1 \end{bmatrix}$ and $C(t) = [c_1(t) \quad c_2(t)]$.

Note that (3) is a linear, time-varying and T-periodic model, with $T = 2\pi$. Next section is devoted to presenting the results of the experiments that we performed to validate the model.

3 Experimental Validation of the Cantilever Model

The device we have used in our experimental setup was a $200\mu m \times 50\mu m \times 2\mu m$ highly doped polysilicon cantilever, fabricated using the MUMPS/CRONOS process, and with a gap between the electrodes of about $2\mu m$. Fig.2 is a SEM picture of the actual device. The cantilever used for testing was isolated from the array by physically removing all the other beams. The mechanical response of the cantilever

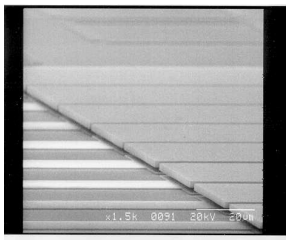

Figure 2: SEM image of a polySi array of cantilevers. Each beam measures $200\mu m \times 50\mu m \times 2\mu m$.

Proceedings of the American Control Conference
Denver, Colorado June 4-6, 2003

was tested in vacuum ($p = 8mT$), using laser vibrometry [16] to measure its displacement and velocity near the free end, when electrostatically driven with different AC voltage signals.

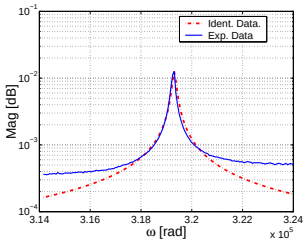

Figure 3: Frequency response of the capacitive cantilever: the dashed line corresponds to measured data, the solid one is its least square fit.

The first experiments we performed aimed at identifing the system as a simple mass-spring-damper model. As a matter of fact, when the amplitude V_o of the AC actuation voltage is small enough, the coefficient q in equation (1) is negligible, and the beam can be described approximately by an ordinary second order differential equation. Fig.3 shows the magnitude, both measured and identified, of the frequency response of this model, excited by a square-rooted sinusoidal signal. A least square fitting of the data gives a resonant frequency of approximately $f_r = 50800Hz$, a damping coefficient $c = 2.1 \times 10^{-4}$, while the quality factor $Q = 2200$ turns out, as expected, to be quite high. The values of these parameters were confirmed by time domain identification experiments as well. If we consider that the Young's modulus for Cronos' polysilicon is $E = 158 \pm 10\,GPa$, its density is $\rho = 2300Kg/m^3$, we can infer from the identified data that the effective length of the capacitor plate is about $L = 160\mu m$.

As the amplitude of the driving signal increases, so does the value of q and this approximation of the model is no longer appropriate. Therefore, we have to return to the original equation (1).

3.1 The Mathieu equation and Parametric Resonance

An extensive literature exists on the standard form of the Mathieu equation,

$$z'' + (a - 2q\cos 2t)z = 0, \qquad (4)$$

that was first introduced by Mathieu to model the vibrational modes of a stretched membrane having an elliptical boundary.

Its stability properties have been thoroughly investigated as a function of a and q. By means of perturbation analysis methods, it is possible to determine the values of these parameters that correspond to unstable behavior. Indeed, the a-q parameter space of (4) can be sub-divided into stable/unstable regions, having a characteristic tongue-like shape [9] (see Fig.4). In particular, and we omit here the details for the sake of brevity, it is not difficult to prove that instabilities occur at $a = n^2$, $n \in \mathbb{N}$. In terms of the

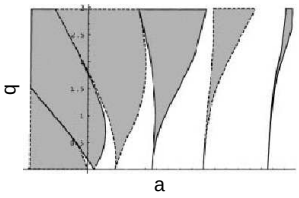

Figure 4: Mathieu equation: the shaded areas correspond to unstable behavior.

physical parameters of the device, the driving frequencies that cause unstable responses in the system are given by

$$\omega_o \approx \frac{2\omega_r}{n} \qquad n \in \mathbb{N},$$

when using a square-rooted sinusoidal driving signal. Similarly, the boundaries of the first instability region, given by $a = 1 \pm q$ for (4), in terms of frequency and amplitude of excitation turn out to be defined by

$$\omega_o^2 = 4\omega_r^2 - 4(1 \mp \frac{1}{2})\frac{\epsilon A V_o}{md^3}.$$

It is worth noting at this point that the presence of a damping term, whose existence we have neglected so far, has the effect of shifting the tongues upwards in the a-q parameter space. In our setup this is of little consequence, because the magnitude of the shift is quite small (order of few mV). However this is not always the case and in fact it is the reason why parametric resonance is difficult to observe at the macroscale. Fig.5 is a comparison between the experimen-

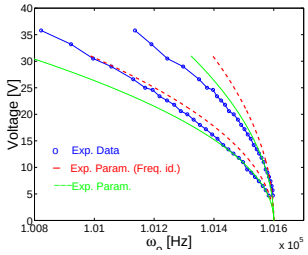

Figure 5: First instability region: experimental data points (circles) and curves with identified parameters.

tal data relative to the boundaries of the first instability region, and the same curves obtained from two sets of parameters: the solid (green) lines come from fitting these experimental data points, the dash-dotted (red) ones come from the frequency response identification.

Inside the instability region the cantilever oscillation does not grow unbounded, as predicted from the previous linear analysis. In reality, physical limiting nonlinear effects always come into play and cause the system to settle down into a steady state response [13]. Here we can attribute the appearance of a nonlinear term in our equation to the large displacements of the beam. As a consequence, the linear spring model needs to be corrected adding a cubic stiffness term.

What we really see when driving the cantilever in parametric resonance regime is a subharmonic 2:1 oscillation of the

beam [13], which vibrates at half the frequency of excitation, as shown in Fig.6, which reproduces data collected from the oscilloscope. Note also that during the transi-

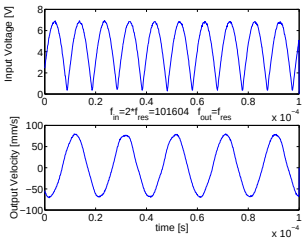

Figure 6: Cantilever response in parametric resonance (oscilloscope data).

tion from non-parametric to parametric region, the response shows a characteristic exponential growth (see Fig.7).

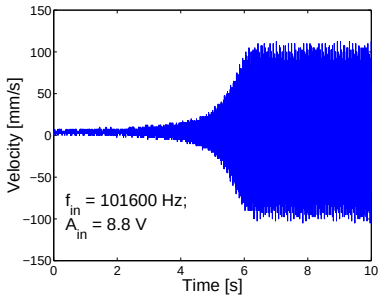

Figure 7: Exponential growth of oscillation following parametric excitation.

Above the critical driving voltage amplitude, and for driving frequencies near the first parametric resonance, the response of the cantilever has the shape depicted in Fig.8. The two curves reproduced in the picture represent the data collected by sweeping the frequency from low to high (blue '+' points) and from high to low (red 'o' points), as indicated by the arrows. This kind of plot is typical of oscillators having a cubic nonlinearity (Duffing). What is worth pointing out here is the sharp transition of the output response (vertical segment of '+' data) that marks the entrance into the parametric region. Since this transition always occurs for the same value ω_1, related to the resonant frequency of the beam, the phenomenon has potentially many applications, from the realization of mechanical filters to extremely sensitive mass sensors. Inside the parametric region, where the periodic subharmonic solution is stable, as the driving frequency increases, the output amplitude starts to decrease, untill it goes back to zero upon exiting the region. The size of the interval $[\omega_1\ \omega_2]$ corresponds to the width of the parametric region represented in Fig.5 for the input amplitude value considered. If we invert the process and start decreasing the frequency, the output amplitude, which is zero at the beginning, starts to increase as soon as we enter the parametric region. This subharmonic periodic solution remains stable even after leaving the region and its amplitude keeps increasing. However, it is only a matter of time before it collapses to the other stable (zero) solution [13]. The location of this second jump is not predictable and depends on the amplitude of the frequency decrements.

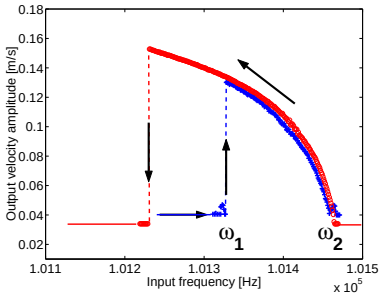

Figure 8: Frequency response above critical driving voltage amplitude ($A = 10V$). The solid and dashed lines have been added to the experimental data points (marked with 'o' and '+') to facilitate the reading.

4 The Optimal Observer Problem

In this section we address the problem of designing a dynamical system capable of providing an estimate $\hat{x}$ for the cantilever displacement, based on the measurement of the current generated. This approach to sensing is particularly advantageous from the point of view of implementation, as it requires a simpler circuitry. As a matter of fact, the extraction of the desired information is left to a software elaboration of the measurements.

As already pointed out in [12], the observer problem can be formulated in the LFT framework as an $\mathcal{H}_\infty$ filtering problem, by defining the variable $z = x - \hat{x}$ (estimation error), and considering the generalized plant (see Fig.9)

$$G_{gen} := \left[\begin{array}{c|cc} \mathrm{A(t)} & \mathrm{[M\ \ 0]} & 0 \\ \hline \mathrm{I} & 0 & \mathrm{-I} \\ \mathrm{C(t)} & \mathrm{[0\ \ N]} & 0 \end{array}\right] = \left[\begin{array}{c|cc} \mathrm{A(t)} & B_1 & 0 \\ \hline C_1 & 0 & D_{12} \\ C_2(t) & D_{21} & 0 \end{array}\right], \tag{5}$$

where the exogenous input $w = [d\ \ n]^T$ represents process and measurement noise, the matrices $A(t)$, $C(t)$ are as in (3) and the input $u = \hat{x}$ is the output of the observer system.

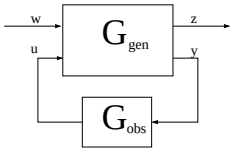

Figure 9: A schematic of the observer problem.

In this framework the optimal observer problem amounts to finding a dynamical system G_{obs} such that the $\mathcal{H}_\infty$ norm of the transfer function T_{zw} from w to z is minimized. If the system is time-invariant, and has the structure of (5), it can be proved that G_{obs} is a Luenberger observer, whose gain L comes from the solution of an appropriate algebraic Riccati equation.

It turns out [11] that the same holds true in the time varying case, where the algebraic equation is replaced by a differential Riccati equation. As a matter of fact, if the periodic non-negative definite solution of this equation, $P(t)$, is stabilizing, the optimal filter is an observer given by

$$\dot{\hat{x}} = A(t)\hat{x} + P(t)C(t)'[y(t) - C(t)\hat{x}].$$

The idea of the method we propose is to use the driving

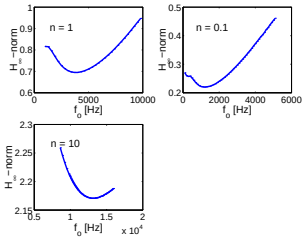

Figure 10: H_∞-norm vs. frequency of excitation.

frequency ω_o as a design parameter and tune its value so that the closed loop system has the minimum attainable H_∞ norm. Fig.10 describes the dependence of this norm from the frequency of excitation, ω_o. The parameters of the cantilever used in this analysis are those indicated in the previous Section. In particular, for the length we have used its effective value, obtained by identification. Notice that the minimum is reached at different values of the driving frequency, depending on the measurement noise weight n. Even though we have no insight to offer at this point in terms of a physical explanation of this result, it is clear that by choosing the value for the driving frequency according to the results of this analysis, we can provide our system with the best combination of parameters to make it more easily observable.

5 The reduced order observer

A reduced order observer allowes us to exploit the information about the state of the system that is provided by the output signal and leave to the observer the task of estimating a smaller portion of the state vector. We refer the interested reader to any book on linear systems theory for the details of this standard technique.

After the appropriate state transformation, which in this case is time varying, the equations of the observer can be written as

$$\begin{aligned}\dot{\hat{v}} &= (A_{11}(t) + L(t)A_{21}(t))\hat{v} + M(t)y \\ \hat{x} &= T(t)\begin{bmatrix} \hat{v} - L(t)y \\ y \end{bmatrix},\end{aligned}$$

where A_{11}, A_{21}, M are π-periodic matrices that can be computed from the system matrices in (3). $L(t)$ is the design parameter, through which we can adjust the behavior of the observer.

First of all, it is obvious that $L(t)$ needs to be chosen so that the state estimation error is asympotically stable. For a T-periodic system this is equivalent to say that its characteristic multipliers, which are the eigenvalues of the state transition matrix Φ computed at T, are in norm less than 1, $|\lambda(\Phi(T))| < 1$. Since we are dealing with a scalar system, $\Phi(T)$ can be easily computed

$$\Phi(T) = e^{\int_0^T (A_{11}+LA_{21})(\sigma)d\sigma},$$

and the condition on the characteristic multipliers is equivalent to the condition $\int_0^T (A_{11}+LA_{21})(\sigma)d\sigma < 0$. By taking $L(t) = k\cos(2t+\phi)$ it can be seen that the stability condition becomes $c/2 + kd_4\pi\cos\phi > 0$, where c is the damping coefficient of (1) and d_4 is a known function of the system parameters. This of course poses a constraint on the choice of k and ϕ. Figure (11) shows the results from a simulation for two admissible values of k and $\phi = 0$: as expected the error dynamics are asymptotically stable. Notice that the variable τ corresponds to a scaled time, therefore the convergence is actually faster than it seems.

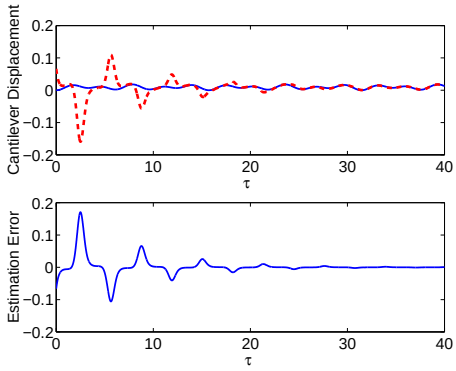

Figure 11: Performance of the reduced order observer in the presence of measurement noise and initial estimation error. The solid line is the cantilever displacement, the dashed line its estimate.

However, we want to select the parameters of this observer not only to ensure stable error dynamics, but also to optimize its performance, with the $\mathcal{H}_\infty$-norm as its measure.

The computation of the $\mathcal{H}_\infty$-norm of a periodic system, as our closed loop system is, represents a difficulty. We have overcome it by using lifting [4] and fast-sampling [2] techniques. In fact it has been proven in [2] that as the sampling rate, N/T T period of the system, grows the approximate sampled model converges to the original one with a rate of $1/N$.

Figure (12) depicts the value of the closed loop norm as k and ϕ vary in $\mathbf{R}$ and $[0 \quad 2\pi)$ respectively. Based on this plot, a better informed choice of k and ϕ turns out to be $k = 0.001$ and $\phi = 3.63$, which give $\mathcal{H}_\infty$-norm=45.

6 Conclusions

In this paper we have derived a mathematical model for an electrostatically actuated microcantilever. In our setup, the microcantilever constitutes the movable plate of a capacitor and its displacement is controlled by the voltage

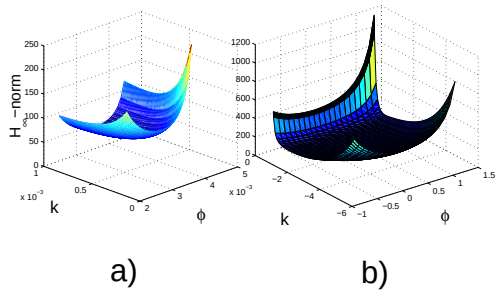

Figure 12: Estimation error for different values of the observer gain: a) $k > 0$ $\cos(\phi) < 0$, b) $k < 0$ $\cos(\phi) > 0$.

applied across the plates. The current generated is used as the sensing signal. In the case of sinusoidal excitation, we have proved that its dynamics are regulated by a special second order differential equation with periodic coefficients, the Mathieu equation. We have provided experimental validation of the mathematical model, which included the mapping the first region of instability of the Mathieu equation. We have formulated the optimal observer problem for the single cantilever and used this design to select the frequency of excitation that makes our model more easily observable. Moreover, it has been used as a benchmark to compare the performance of a reduced order observer and tune its parameters. The extension of these results to the array configuration is the subject of our current research.

Acknowledgements

The first author would like to thank Wenhua Zhang and Rajashree Baskaran for the precious help offered during the testing of the device.

This work partially supported by a National Science Foundations grant ECS-0226799.

References

[1] P. Attia, M. Boutry, A. Bosseboeuf and P. Hesto, "Fabrication and Characterization of Electrostatically Driven Silicon Microbeams", *Microelectronics J.*, 29, pp. 641-644, 1998.

[2] B. Bamieh, M.A. Dahleh and J.B. Pearson,"Minimization of the L^{∞}-Induced Norm for Sampled-Data Systems," *IEEE Trans. on AC*, Vol. 38, No. 5, pp. 717-732, May 1993.

[3] N. Blanc, J. Brugger, N.F. de Rooji and U. Durig, "Scanning Force Microscopy in the Dynamic Mode Using Microfabricated Capacitive Sensors", *J. Vac. Sci. Technol. B*, 14(2), pp.901-905, Mar/Apr 1996.

[4] T. Chen and B. Francis, "Optimal Sampled-Data Control Systems", Springer, 1995.

[5] B.W. Chui, T.W. Kenny, H.J. Mamin, B.D. Terris and D. Rugar, "Independent Detection of Vertical and Lateral Forces with a Sidewall-Implanted Dual-axis Piezoresistive Cantilever", *Appl. Phys. Lett.*, Vol. 72, No.11, pp.1388-1390, March 1998.

[6] P. Gaucher, D. Eichner, J. Hector and W. von Munch, "Piezoelectric Bimorph Cantilever for Actuationf and Sensing Applications", *J. Phys. IV France*, Vol. 8, pp. 235-238, 1998.

[7] Q.A. Huang and N.K.S. Lee, "A Simple Approach to Characterizing the Driving Force of Polysilicon Laterally Driven Thermal microactuators", *Sensors and Actuators*, 80, pp. 267-272, 2000.

[8] T. Itoh, T. Ohashi and T. Suga, "Piezoelectric Cantilever Array for Multiprobe Scanning Force Microscopy", *Proc. of the IX Int. Workshop on MEMS*, San Diego, CA, USA, 11-15 Feb. 1996. Mew York, MY, USA: IEEE, 1996. pp. 451-455.

[9] N.W. McLachlan, "Theory and Applications of the Mathieu Functions", *Oxford Univ. Press*, London, 1951.

[10] S.C. Minne, S.R. Manalis and C.F. Quate, "Parallel Atomic Force Microscopy Using Cantilevers with Integrated Piezoresistive Sensors and Integrated Piezoelectric Actuators", *Appl. Phys. Lett.*, Vol. 67, No. 26, pp. 3918-3920, 1995.

[11] K. Nagpal and P. Khargonekar, "Filtering and Smoothing in an H_{∞} Setting", *IEEE Trans. on Automatic Control*, Vol. 36, No. 2, February 1991.

[12] M. Napoli, B. Bamieh, "Modeling and Observer Design for an Array of Electrostatically Actuated Microcantilevers", in *Proc. 40'th IEEE Conference on Decision and Control*, Orlando, FL, December 2001.

[13] R. Rand, "Lecture Notes on Nonlinear Vibrations, available online at *http://www.tam.cornell.edu/randdocs/*.

[14] Y. Shiba, T. Ono, K. Minami and M. Esashi, "Capacitive AFM Probe for High Speed Imaging", *Trans. of the IEE of Japan*, Vol. 118 - E, No.12, pp. 647-650, 1998.

[15] M. Tortonese, R.C. Barrett and C.F. Quate, "Atomic Resolution with an Atomic Force Microscope Using Piezoresistive Detection", *Appl. Phys. Lett*, Vol. 62, pp. 834-836, 1993.

[16] K. Turner, "Multi-Dimensional MEMS Motion Characterization using Laser Vibrometry",in *Transducers '99 - 10th International Conference on Solid-State Sensors and Actuators, Digest of Technical Papers*, Sendai, Japan, June 1999.